

# Angular and frequency dependence of standing spin waves in FePt films

D. M. Jacobi, E. Sallica Leva, N. Álvarez, M. Vásquez Mansilla, J. Gómez, and A. Butera

Citation: Journal of Applied Physics 111, 033911 (2012); doi: 10.1063/1.3682104

View online: http://dx.doi.org/10.1063/1.3682104

View Table of Contents: http://scitation.aip.org/content/aip/journal/jap/111/3?ver=pdfcov

Published by the AIP Publishing

# Articles you may be interested in

Spin waves and small intrinsic damping in an in-plane magnetized FePt film Appl. Phys. Lett. **101**, 222402 (2012); 10.1063/1.4768787

Magnetic anisotropy and spin wave relaxation in CoFe/PtMn/CoFe trilayer films

J. Appl. Phys. 105, 073910 (2009); 10.1063/1.3093927

Ultrafast optical study of spin wave resonance and relaxation in a CoFe/PtMn/CoFe trilayer film

J. Appl. Phys. 105, 07D304 (2009); 10.1063/1.3063675

FePt films fabricated by electrodeposition

J. Appl. Phys. 101, 09K519 (2007); 10.1063/1.2711810

The mechanism of Ag top layer on the coercivity enhancement of FePt thin films

J. Appl. Phys. 97, 10H502 (2005); 10.1063/1.1854332



TREK, INC. 190 Walnut Street, Lockport, NY 14094 USA • Toll Free in USA 1-800-FOR-TREK • (t):716-438-7555 • (f):716-201-1804 • sales@trekinc.com

# Angular and frequency dependence of standing spin waves in FePt films

D. M. Jacobi, <sup>1</sup> E. Sallica Leva, <sup>2</sup> N. Álvarez, <sup>2</sup> M. Vásquez Mansilla, <sup>2</sup> J. Gómez, <sup>2</sup> and A. Butera<sup>2,3,a)</sup>

(Received 31 August 2011; accepted 4 January 2012; published online 9 February 2012)

We present a detailed analysis of the dynamic response of the magnetization in as-made FePt thin films, particularly studying the angular dependence of standing spin waves that can be observed when the external field is applied close to the film normal. We have found that the field separation between the uniform and the first excited mode depends strongly on angle and microwave frequency. To explain the observed behavior we have adopted the surface inhomogeneity model in the circular precession approximation. Using this model the experimental data could be very well fitted assuming that spins are not totally pinned at the surfaces by introducing a finite surface anisotropy. The experimental angular behavior of the resonance field at three different frequencies could be fitted with a single set of parameters indicating that the reported changes in the surface anisotropy as a function of film thickness are intrinsic to the samples. © 2012 American Institute of Physics. [doi:10.1063/1.3682104]

#### I. INTRODUCTION

In the last years equiatomic FePt alloys have been intensively studied in different confined forms in which one or more dimensions are reduced to the nanometer scale. <sup>1–4</sup> Particularly, metastable disordered FCC thin films, phase which generally forms when films are fabricated at room temperature, present a very rich variety of magnetic properties. Despite not having a large magnetocrystalline anisotropy or a high coercivity as the ordered phase, these films show a relatively small uniaxial effective anisotropy perpendicular to the film plane ( $K_{\perp} \sim 1.5 \times 10^6 \text{ erg/cm}^3$ ). The origin of this out-of-plane anisotropy is due to the combined effects of magnetocrystalline anisotropy (samples grow with a [111] texture perpendicular to the film plane)<sup>5</sup> and magnetoelastic energy (as-deposited films form under in-plane compressive stress which induces a perpendicular easy axis).

Disordered FePt thin films, and also similar alloys like FePd and CoPt, often show a stripe-like magnetic domain structure. This kind of magnetic structure is due to the presence of a uniaxial perpendicular anisotropy which competes with the demagnetizing energy. It is generally observed that below a critical thickness,  $d_{\rm cr}$ , that depends on the so-called Q-factor,  $Q = K_{\perp}/2\pi M_s^2$ , the magnetization lies in the plane of the film. Thicker films, on the other hand, present a small out-of-plane component of the magnetization which periodically changes from the "up" to the "down" direction inducing the formation of a stripe structure. Values of the critical thickness are in the range of 20–30 nm for FePt (Refs. 1 and 5) and also for FePd.

Ferromagnetic resonance in these alloys have been reported either in the saturated <sup>7–12</sup> or the unsaturated state. <sup>13</sup>

Apart from the uniform resonance mode, several additional lines have been observed in thin films. These absorptions have been attributed to standing spin waves, <sup>7,9,12</sup> domain mode ferromagnetic resonance (FMR) corresponding to FMR within domains, <sup>8</sup> and domain wall resonances due to collective modes of domain wall vibrations. <sup>8</sup>

Our group has previously reported the observation and the analysis of additional resonance lines in a set of disordered FePt films that were assigned to standing spin waves (SSW). 10,12 From those studies it was possible to establish that a single value of the perpendicular anisotropy  $K_{\perp}$  and the exchange stiffness constant A could be used to describe the thickness behavior of all studied films. However, we observed variations of the surface anisotropy  $K_S$  and a change of the magnetization in the presurface layer  $\partial_n M$ , which needed to be further studied in order to elucidate the reasons for these changes with the film thickness. We present in this work FMR studies in a set of thin films with thicknesses in the range 28–100 nm focusing the attention on the analysis of the angular and frequency dependence of the SSWs. In this case, the dynamic response of the samples has been measured at three different frequencies and the angular behavior of the SSW spectra close to the film normal was carefully analyzed. Results, modeling, and conclusions are presented in the following sections.

# II. EXPERIMENTAL DETAILS

The films used in this study are the same samples that we have used for the FMR experiments in Ref. 12. In short, as-made disordered FePt films have been fabricated by dc magnetron sputtering on naturally oxidized Si (100) substrates. The samples were deposited from an FePt alloy target with a nominal atomic composition of 50/50. The chamber was pumped down to a base pressure of  $10^{-7}$  Torr and the films were sputtered using 2 mTorr of Ar pressure, a

<sup>&</sup>lt;sup>1</sup>Universidad Tecnológica Nacional, 3100 Paraná, Entre Ríos, Argentina

<sup>&</sup>lt;sup>2</sup>Centro Atómico Bariloche (CNEA), 8400 Bariloche, Río Negro, Ārgentina

<sup>&</sup>lt;sup>3</sup>Instituto Balseiro (U. N. Cuyo), 8400 Bariloche, Río Negro, Argentina

a) Author to whom correspondence should be addressed. Electronic mail: butera@cab.cnea.gov.ar. Also at: Consejo Nacional de Investigacions Científicas y Técnicas, Argentina.

power of 20 W, and a target-substrate distance of 5 cm. With these parameters we obtained a sputtering rate of 0.15 nm/s. Eight different films were sputtered with thicknesses of 9, 19, 28, 35, 42, 49, 56, and 94 nm. X-ray diffractograms indicated that as-made samples tend to grow with a high [111] texture normal to the film plane and that they are under an in-plane compressive stress. These two effects tend to produce an effective perpendicular anisotropy  $K_{\perp} = 1.5(4)$  $\times$  10<sup>6</sup> erg/cm<sup>3</sup>. The average grain size estimated from transmission electron microscopy (TEM) micrographs is  $\langle D \rangle \sim 4$ nm. This value is smaller than the so-called exchange length due to the perpendicular anisotropy  $^{14}$   $L = \sqrt{A/K_{\perp}}$ , which for films with atomic disorder is  $L \gtrsim 7$  nm. For this reason the magnetic response of individual grains is coupled by the exchange interaction and a single, relatively narrow, resonance line is then expected for the uniform resonance mode. The saturation magnetization, the exchange stiffness constant and the Q-factor of these samples have been already reported in Refs. 5 and 12 with the following values:  $M_s = 866(25)$  $emu/cm^3$ ,  $A \sim 0.95 \times 10^{-6}$  erg/cm, Q = 0.32(8). FMR spectra have been acquired at room temperature with a commercial Bruker ESP 300 spectrometer at frequencies of 9.5 GHz (X-band), 24.1 GHz (K-band), and 35 GHz (Q-band). The samples were placed at the center of a resonant cavity where the derivative of the absorbed power was measured using a standard field modulation and lock-in detection technique with amplitudes in the range 5-20 Oe. The film plane was in all cases parallel to the excitation microwave field. Angular variations with respect to the external dc field were made around the film normal in an angular range of approximately  $\pm 10^{\circ}$ . The maximum available dc field was 22 kOe.

## III. EXPERIMENTAL RESULTS AND MODEL

In Ref. 12 we have reported the angular dependence of the resonance spectra at the X-band for the case in which the external field was varied from the in-plane toward the film plane normal. We have found that a single resonance line was always observed for the in-plane configuration while one or more additional absorptions could be observed when the field H was applied near a direction perpendicular to the film plane, at least in the samples with  $d \ge 28$  nm. In this study we have carefully measured the angular variation of the field separation between the main or uniform mode ( $H_{r0}$ ) and the first additional absorption ( $H_{r1}$ ) also at K- and Q-bands.

The detailed theory of ferromagnetic resonance can be read in the book of Gurevich and Melkov. <sup>15</sup> In our case nonzero wave vectors are introduced into the dispersion relation in order to account for nonuniform precession modes,

$$\left(\frac{\omega}{\gamma}\right)^{2} = \left[H_{rn}\cos(\phi - \phi_{H}) - H_{eff}\cos^{2}(\phi) + \frac{2A}{M}k_{n}^{2}\right] 
\left[H_{rn}\cos(\phi - \phi_{H}) - H_{eff}\cos(2\phi) + \frac{2A}{M}k_{n}^{2}\right], \tag{1}$$

where  $\omega$  is the angular frequency of the precession of the magnetization vector,  $\gamma = g\mu_B/\hbar$  is the gyromagnetic ratio,  $H_{rn}$  is the resonance field for the mode n,  $H_{eff} = 4\pi M_s$ 

 $-2~K_{\perp}/M_s$  is the effective anisotropy field,  $k_n$  is the wave vector for mode n, and  $\phi$  and  $\phi_H$  are the angles that the magnetization and the external field form with the film normal. The wavevector  $k_n$  is assumed to be zero for n=0 and the first excited mode is assigned to n=1. As explained in Ref. 12, the experimental data can be well described using the surface inhomogeneity (SI) model. The SI model considers a finite pinning for the spins located at the surfaces and solves Eq. (1) in the single wave vector and circular precession approximation regime (only the real solution of  $k_n$  is considered). With adequate boundary conditions it is possible to estimate the associated surface pinning parameter, p, by using the relationship between the wave vector  $k_n$  and the parameter p,

$$\tan(k_n d) = \frac{2k_n p}{k_n^2 - p^2}.$$
 (2)

In the Kittel model (that assumes infinite pinning at the film surfaces) the wavevector  $k_n = n\pi/d$  and does not depend on the angle  $\phi$ . However, in the SI model both  $k_n$  and p may depend on the orientation of the magnetization with respect to the film normal. We have plotted in Fig. 1 the two functions of the wavevector  $k_n$  that result from Eq. (2) for a fixed d value and  $\phi_H = 0$  to illustrate this effect. Experimentally the wavevector  $k_n$  can be deduced from Eq. (1) so that two values of p can be obtained by using Eq. (2). If the parameter p is known, the wavevector could then be obtained numerically from the intersection between both curves. In all our analysis we have centered our attention in the first excited mode n = 1 because the others have negligible intensities or are out of the available microwave excitation frequency. For this reason we will omit the subscript n of the wavevector

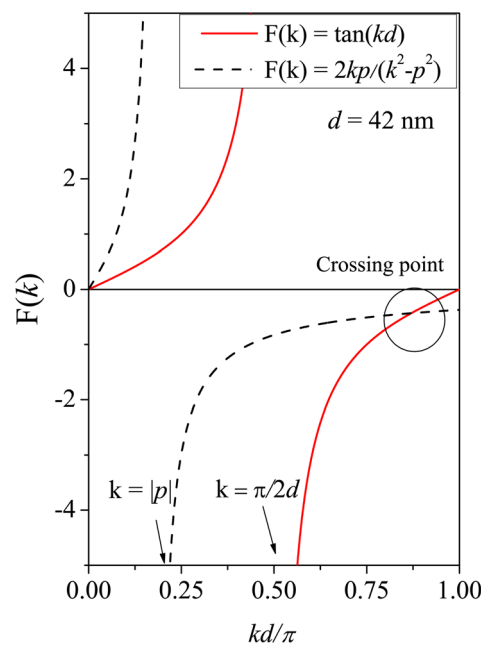


FIG. 1. (Color online) Functions  $F(k) = \tan(kd)$  and  $F(k) = 2kp/(k^2 - p^2)$  from Eq. (2), plotted as a function of the normalized wavevector  $kd/\pi$ . The intersection between both curves can be used to estimate the pinning parameter p or the wave vector k. No solutions for n = 1 are obtained if  $\pi/2d < |p| < 3\pi/2d$ .

from now on and call it simply k. Analyzing Eq. (2) and Fig. 1 we can see that the  $F(k) = \tan(kd)$  curve has an asymptote at  $k = \pi/2d$  while  $F(k) = 2kp/(k^2 - p^2)$  diverges at k = |p|. By a simple inspection of the curves it is easy to realize that there is an intersection point (different than zero) only if  $|p| < \pi/2d$  or  $|p| > 3\pi/2d$ .

The pinning parameter and the angle of equilibrium of the magnetization vector,  $\phi$ , are phenomenologically related with magnetic properties of the film in the SI model<sup>17</sup> through the relationship,

$$p = -\frac{K_s}{A}\cos(2\phi) - \frac{\partial_n M}{M},\tag{3}$$

where  $K_s$  is the surface anisotropy, A the exchange stiffness constant, and  $\partial_n M$  the change of the magnetization in the normal direction at the presurface area. Consequently both p and k are strongly dependent functions of the angle  $\phi$  and their values will change when the magnitude or the orientation of the external magnetic field is varied. The simplest form for the surface anisotropy is to assume an easy anisotropy axis, so that the free energy is of the form  $F_s = K_s \cos^2 \phi \sin^2 \theta$ . If  $K_s < 0$  the easy axis is normal to the film plane (parallel to  $\hat{x}$ ) and for  $K_s > 0$  the surface energy is minimized if M is within the film plane (the plane yz is an easy anisotropy plane).

Figure 2 shows the predicted evolution of  $\cos(2\phi)$ , p, and k as a function of the external magnetic field for two different values of  $\phi_H$ . If the angle  $\phi_H$  is kept fixed, for example, at  $\phi_H = 0^\circ$  or  $\phi_H = 5^\circ$  the equilibrium angle of the magnetization vector  $\phi$  tends to align with H when the field is increased. In all frequencies the resonance field for  $\phi_H = 0$  occurs when  $\phi = 0$  and the same value of p and k is expected for all frequencies. However, when the field is not applied

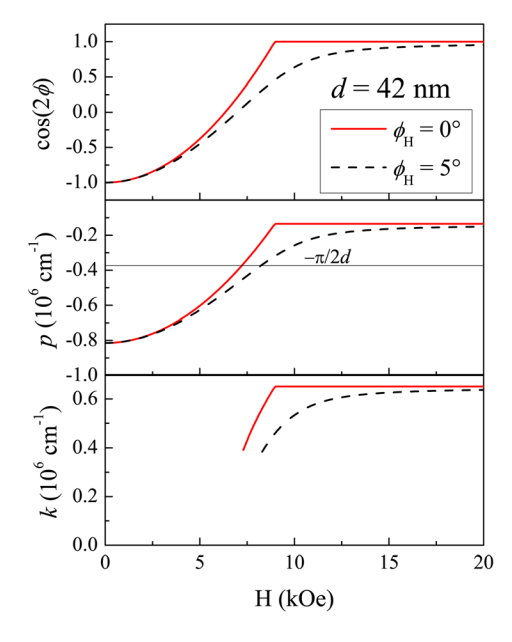


FIG. 2. (Color online) Evolution of  $\cos(2\phi)$ , p and k as a function of the external magnetic field in the cases  $\phi H=0^\circ$  and  $\phi H=5^\circ$ . When the field increases the angle of equilibrium  $\phi$  changes from  $\pi/2$  to 0 and consequently the values of p and k reach a constant value. A sharp transition is only observed for  $\phi H=0^\circ$ . Note that when  $\pi/2d < |p| < 3\pi/2d$ , Eq. (2) is no longer fulfilled for any value of k.

normal to the film plane, the equilibrium angle of the magnetization depends on the magnitude of H. Larger excitation frequencies imply larger resonance fields and as a consequence the misalignment between  $\phi_H$  and  $\phi$  is more pronounced in X-band than in the higher frequencies. This variation of  $\phi$  with  $\phi_H$  and H produces the field dependence of p and k that can be observed in Fig. 2 and indicates that the effective pinning is different for each value of  $\phi$ . This behavior is known as dynamical pinning<sup>21</sup> and is responsible for the variation of the wave vector k when  $\phi_H \neq 0$ . Note that when p is in the range  $\pi/2d < |p| < 3\pi/2d$ , Eq. (2) is no longer fulfilled for any value of k.

From the measured spectra we have obtained the field separation between the uniform mode and the first excited mode as a function of the angle  $\phi_H$  in a small region around  $\phi_H = 0$ . The experimental results are plotted in Fig. 3 for the whole set of samples (with  $d \ge 28$  nm) at the different excitation frequencies. As predicted by Eq. (1) and considering the experimental error, the field separation at  $\phi_H = 0$  is the same for the three different frequencies and decreases when the film thickness increases because of the 1/d-like dependence of k. As can be seen in the figure the observed results are totally consistent with the expected behavior. When  $\phi_H$  is moved away from the film normal, the difference  $H_{r0} - H_{r1}$  has a different angular variation depending on the frequency and the thickness of the sample.

In order to understand this angular evolution we can explore the dispersion relation given by Eq. (1) at angles close to the film normal (see Fig. 4). In the figure we present the calculated dispersion relation for a film of 42 nm at the angles  $\phi_H = 0^\circ$  and  $\phi_H = 5^\circ$  using as parameters the values of  $K_s$ ,  $\partial_n M$ , and  $H_{eff}$  given in Table I. In the perpendicular orientation the separation  $H_{r0} - H_{r1}$  is, as already discussed, independent of the excitation frequency, at least for

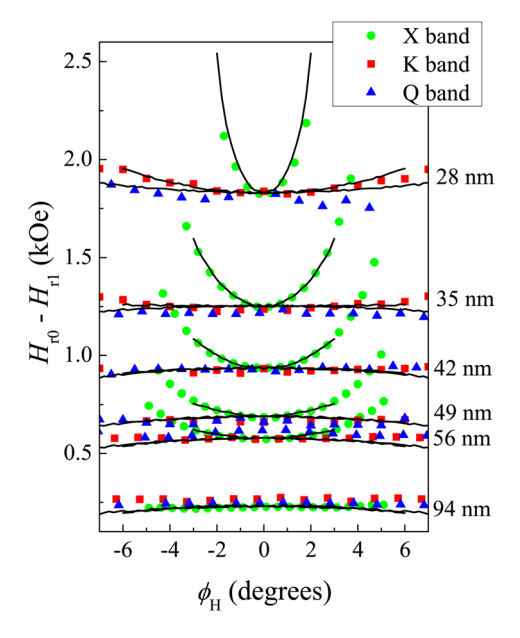


FIG. 3. (Color online) Angular variation close to the film normal of the field separation between the uniform mode and the additional line  $(H_{r0} - H_{r1})$  in samples with a thickness of 28, 35, 42, 49, 56, and 94 nm. Different symbols indicate data measured at X-, K- or Q-bands. Solids lines correspond to the best fit obtained by using the SI model.

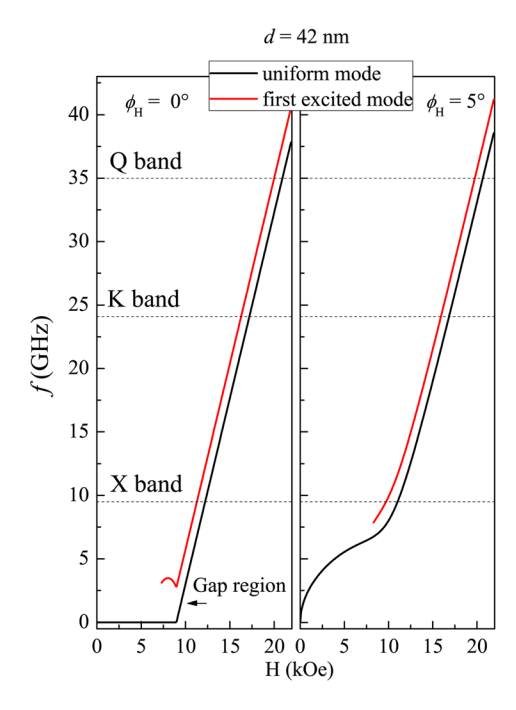


FIG. 4. (Color online) Dispersion relation for film of 42 nm calculated at the angles  $\phi_H = 0^{\circ}$  and  $\phi_H = 5^{\circ}$  using Eq. (1) and the parameters of I.

frequencies larger than  $f \sim 3$  GHz where a gap opens in the dispersion relation of the excited mode. When  $\phi_H$  is moved away from the perpendicular direction the model predicts a different behavior than for  $\phi_H = 0$ . From Eq. (1) it is possible to obtain an approximate expression for the field separation when H is applied close to the film normal,

$$H_{r0} - H_{r1} \sim \frac{2A}{M\cos(\phi - \phi_H)} k^2. \tag{4}$$

In the case of the Kittel model k does not depend on the angle  $\phi_H$  and the field separation is expected to increase as the applied field is moved away from the film normal. On the other hand, if the pinning is dynamic the value of k decreases when  $\phi_H \neq 0$  and then a smaller field separation between  $H_{r0}$  and  $H_{r1}$  is expected. Thinner samples tend to have a large and weakly angle dependent absolute value of the pinning parameter and follow the behavior predicted by Eq. (4) for relatively constant values of k. For this reason the  $H_{r0}-H_{r1}$  versus  $\phi_h$  curves at X-band have a larger curvature than the

TABLE I. Surface anisotropy  $K_s$ , variation of the magnetization at the presurface layer  $\partial_n M$ , and effective field  $H_{eff}$  as a function of the film thickness taken from Ref. 12. These values have been used to fit the experimental data of Fig. 3.

d (nm)	$K_s (\text{erg/cm}^2)$	$\partial_{\rm n} M  ({\rm emu/cm}^3/{\rm nm})$	$H_{eff}$ (Oe)
28	-0.059	29.3	9000
35	-0.232	37.9	8860
42	-0.322	41.0	8970
49	-0.347	41.5	8780
56	-0.390	41.8	8800
94	-0.446	42.5	8720

data measured at K- or Q-bands in the same sample. In the thinnest film in which two signals are detected (d = 28 nm) it is also possible to observe a larger curvature in the K-band data compared to the experiments performed at Q-band. Another distinctive feature, particularly notable in the thinner films and the lower frequencies, is a reduced angular range in which the second mode could be detected. As already mentioned thinner samples have a larger wave vector (k scales with the confinement size, in this case the film thickness), and the frequency gap indicated in Fig. 4 becomes larger when k increases, in particular the frequency gap for the first excited mode is  $f_g = (\gamma/2\pi)(2A/M)k^2$ . For this reason there is a critical angle,  $\phi_{HC}$ , where the gap exceeds the excitation frequency and the resonance condition cannot tune for angles larger than  $\phi_{hc}$ . This behavior explains the very sharp angular variation in the sample of 28 nm at the X-band and the disappearance of the absorption in a region of  $\phi_H = \pm 2^{\circ}$  around the film normal. For simplicity reasons the present model was restricted to the circular precession approximation which works relatively well when the angle  $\phi$  obeys the relationship  $\cos(2\phi) > 0.9$  (as in Ref. 12). This constraint in the magnetization angle is fulfilled if the magnetic field does not deviate more than  $\phi_H \sim \pm 3^{\circ}$ ,  $\pm 6^{\circ}$ , and  $\pm 7^{\circ}$  from the perpendicular direction at X-, K-, and Q-bands, respectively. For this reason the angular range of the solid lines in Fig. 3, that correspond to the best fits within the model, depends on the working frequency.

In the thicker samples the curvature in the angular variation of  $H_{r0}$ – $H_{r1}$  tends to be slightly negative. This behavior cannot be simply deduced from Eq. (4), and is a consequence of the simultaneous variation of k and  $\phi$  in the dynamical pinning regime when the field is moved away from the out-of-plane direction.

The analysis of the angular variation for higher values of the angle  $\phi$  must be carefully performed because the circular precession approximation cannot be applied. This study, however, is beyond the scope of this article.

## IV. CONCLUSIONS

We have done a detailed analysis of the dynamic response of the magnetization in as-made FePt thin films, particularly studying the angular dependence of the field separation between the uniform and the first excited mode at different microwave frequencies.

The peculiar behavior could be very well explained within the SI model in the circular precession approximation, at least for angles close to  $\phi_H = 0$ . We needed to consider that spins are not perfectly pinned at the surfaces by introducing a finite surface anisotropy and a change in the magnetization in the presurface layer. With a single set of parameters it was possible to explain the experimental angular behavior of the resonance field at three different frequencies, including the loss of the signal at a critical angle in the X-band experiments. This is a very good indication that the observed changes in  $K_S$  and  $\partial_n M$  as a function of film thickness are intrinsic to the samples. Investigations in films in which the surface properties are changed in a controlled manner are currently underway.

#### **ACKNOWLEDGMENTS**

This was supported in part by Conicet under Grant No. PIP 112-200801-00245, ANPCyT under Grant No. PICT 2010-0773, and U.N. Cuyo under Grant No. 06/C235, all from Argentina. Technical support from Rubén E. Benavides is greatly acknowledged.

- <sup>1</sup>S. Okamoto, N. Kikuchi, O. Kitakami, T. Miyazaki, Y. Shimada, and K. Fukamichi, Phys. Rev. B 66, 024413 (2002).
- <sup>2</sup>S. Sun, C. B. Murray, D. Weller, L. Folks, and A. Moser, Science 287, 1989 (2000).
- <sup>3</sup>J. M. Vargas, R. D. Zysler, and A. Butera, Appl. Surf. Sci. **254**, 274 (2007). <sup>4</sup>A. Butera, S. S. Kang, D. E. Nikles, and J. W. Harrell, Physica B 354, 108
- <sup>5</sup>E. Sallica Leva, R. C. Valente, F. Martínez Tabares, M. Vásquez Mansilla, S. Roshdestwensky, and A. Butera, Phys. Rev. B 82, 144410 (2010).
- <sup>6</sup>V. Gehanno, R. Hoffmann, Y. Samson, A. Marty, and S. Auffret, Eur. Phys. J. B 10, 457 (1999).
- <sup>7</sup>J. BenYoussef, H. Le Gall, N. Vukadinovic, V. Gehanno, A. Marty, Y. Samson, and B. Gilles, J. Magn. Magn. Mater. 202, 277 (1999).
- <sup>8</sup>N. Vukadinovic, H. Le Gall, J. BenYoussef, V. Gehanno, A. Marty, Y. Samson, and B. Gilles, Eur. Phys. J. B 13, 445 (2000).
- <sup>9</sup>A. Martins, S. C. Trippe, A. D. Santos, and F. Pelegrini, J. Magn. Magn. Mater. 308, 120 (2007).
- <sup>10</sup>M. Vásquez Mansilla, J. Gómez, and A. Butera, IEEE Trans. Magn. 44, 2883 (2008).

- <sup>11</sup>M. Vásquez Mansilla, J. Gómez, E. Sallica Leva, F. Castillo Gamarra, A. Asenjo Barahona, and A. Butera, J. Magn. Magn. Mater. 321, 2941
- <sup>12</sup>E. Burgos, E. Sallica Leva, J. Gómez, F. Martínez Tabares, M. Vásquez Mansilla, and A. Butera, Phys. Rev. B 83, 174417 (2011).
- <sup>13</sup>N. Vukadinovic, M. Labrune, J. BenYoussef, A. Marty, J. C. Toussaint, and H. Le Gall, Phys. Rev. B 65, 054403 (2001).
- <sup>14</sup>J. Stöhr and H. C. Siegmann, Magnetism, From Fundamentals to Nanoscale Dynamics (Springer, Berlin, 2006), p. 514.
- 15 A. G. Gurevich and G. A. Melkov, Magnetization Oscillations and Waves (CRC Press, Boca Raton, 1996).
- <sup>16</sup>Strickly speaking the assignment of n = 0 and n = 1 to the first two modes is not correct because the n = 0 mode can be only excited in the case of uniform magnetization and no surface pinning. If the first mode is n = 1the second can be n=2 or n=3 depending on the symmetry of the pinning. In any case this assignment will produce a shift in the relation between mode separation vs film thickness, but will not affect the overall discussion.
- <sup>17</sup>H. Puszkarski, Prog. Surf. Sci. 9, 171 (1979); P. E. Wigen, Thin Solid Films 114, 135 (1984); Z. Frait and D. Fraitová, Frontiers in Magnetism of Reduced Dimension Systems, NATO ASI Series 3, edited by P. Wigen, VG Bar'yakhtar and N Lesnik (Kluwer Academic Publishers, Dordrecht, 1998), Vol. 49, pp. 121-152.
- <sup>18</sup>J. Gómez, A. Butera, and J. A. Barnard, Phys. Rev. B **70**, 054428
- <sup>19</sup>G. T. Rado and J. R. Weertman, J. Phys. Chem. Solids **11**, 315 (1959).
- <sup>20</sup>A. Maksymowicz, Phys. Rev. B **33**, 6045 (1986).
- <sup>21</sup>P. E. Wigen, C. F. Kooi, M. R. Shananbarger, and Thomas D. Rossing, Phys. Rev. Lett. 9, 206 (1962).